

SUPPLEMENTARY MATERIAL

for

Role of the 5' end phosphorylation state for small RNA stability and target RNA regulation in bacteria

Alexandra Schilder¹ and Boris Görke^{1*}

¹Department of Microbiology, Immunobiology and Genetics, Max Perutz Labs, University of Vienna, Vienna Biocenter (VBC), 1030 Vienna, Austria.

Keywords: Small RNA, RNase E, 5' monophosphate, RNA decay, adaptor protein RapZ.

Short title: Role of sRNA 5' phosphorylation state

*Corresponding author

E-mail: boris.goerke@univie.ac.at

TABLE OF CONTENTS

Supplementary Figures

Supplementary Figure S1. Comparison of target RNA signals in presence of GlmZ'-*gfp* under different inducer combinations.

Supplementary Figure S2. Increasing the distance between GlmZ' and the MicC start nucleotide in the *glmZ'-micC* fusion by one or two nucleotides has no impact on the regulatory performance of the released 5'-MicC species.

Supplementary Figure S3. Mutation of the RNase E cleavage site at position + 9 increases steady state levels of 5'-MicC significantly.

Supplementary Figure S4. Comparison of the regulatory performance of 5'- and 5'PPP-RyhB.

Supplementary Figure S5. Determination of *sodB* decay rates triggered by 5'PPP- and 5'-RyhB and analysis of RyhB stability.

Supplementary Figure S6. Northern blot addressing the precise size of the *nhaB* mRNA.

Supplementary Figure S7. Comparison of gel migration velocities of 5'PPP-CpxQ and CpxQ derived from the GlmZ'-CpxQ fusion with endogenous CpxQ.

Supplementary Figure S8. Analysis of GcvB repression by 5'PPP- and 5'-SroC.

Supplementary Figure S9. Comparison of the regulatory strength of 5'- and 5'PPP-CpxQ in a strain lacking pyrophosphohydrolase RppH.

Supplementary Figure S10. Comparison of the regulatory strength of 5'PPP- and 5'-SroC in a strain lacking pyrophosphohydrolase RppH.

Supplementary Figure S11. Comparison of GcvB decay rates triggered by 5'PPP- and 5'-SroC in a strain lacking pyrophosphohydrolase RppH.

Supplementary Figure S12. Comparison of *ompD* decay rates triggered by 5'PPP- and 5'-MicC in a strain lacking pyrophosphohydrolase RppH.

Supplementary Figure S13. Analysis of *ompD* decay triggered by MicC in *Salmonella* strains synthesizing wild-type RNase E or the RNase E R169K variant.

Supplementary Figure S14. Determination of *ompD* decay rates triggered by 5'PPP- and 5'-MicC in a strain expressing the truncated *rne598* variant.

Supplementary Figure S15. RNA half-life experiments in presence of the GlmZ'-*gfp* fusion RNA to show sRNA-specific target destabilization.

Supplementary Materials and Methods

Construction of plasmids

Supplementary Tables

Supplementary Table I. Bacterial strains used in this study.

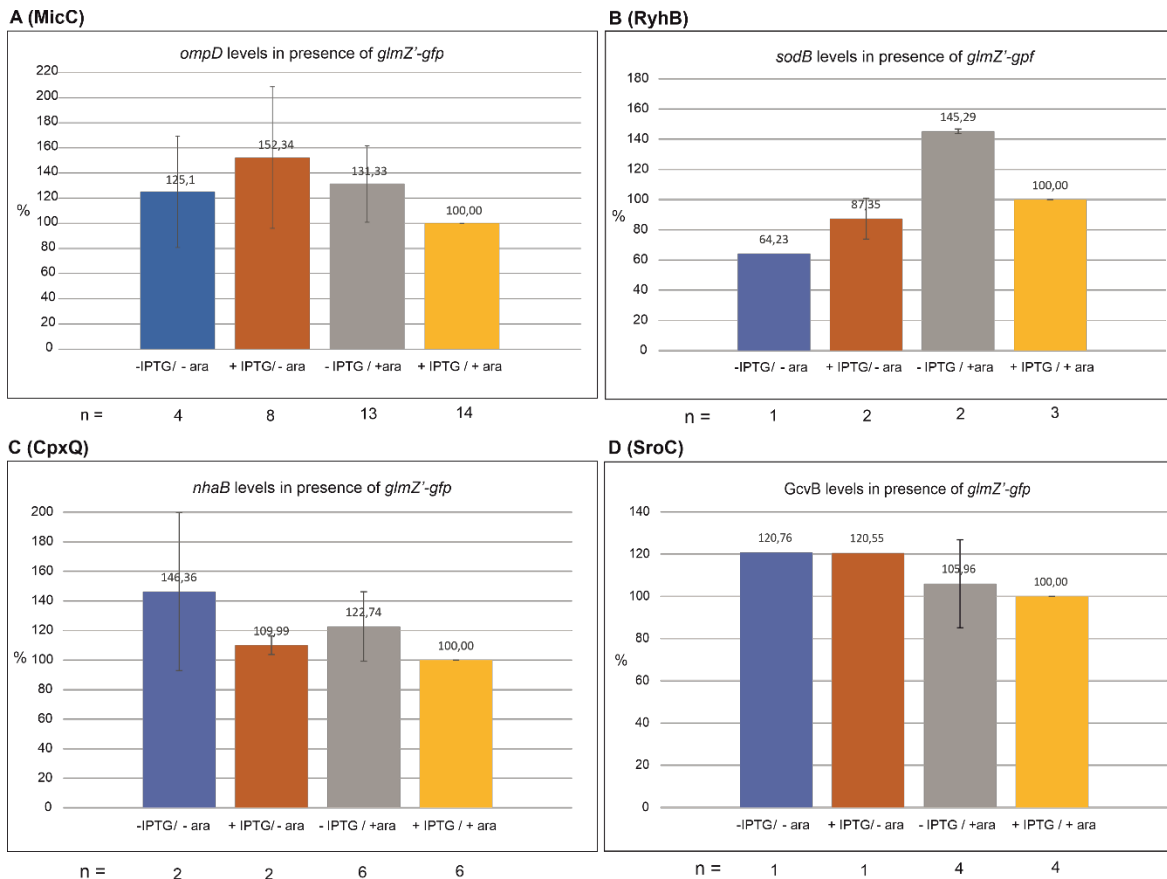
Supplementary Table II. Plasmids used in this study.

Supplementary Table III. Oligonucleotides used in this study.

Supplementary References

SUPPLEMENTARY FIGURES

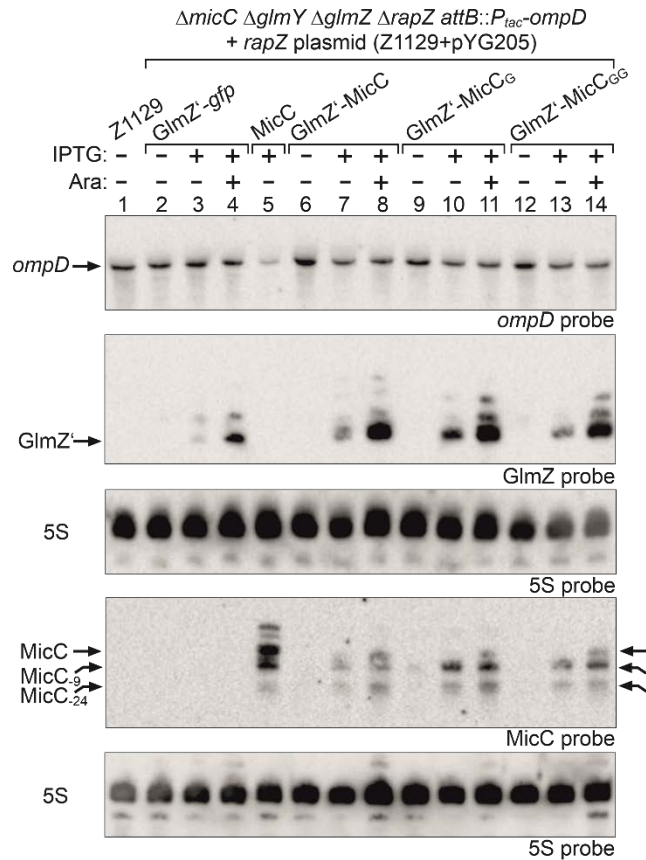
Supplementary Figure S1.



Supplementary Figure S1. Comparison of target RNA signals in presence of *GlmZ'-gfp* under different inducer combinations. For quantification of Northern Blots from steady state experiments, target RNA signals were compared to the average target RNA signal intensities in presence of *GlmZ'-gfp* on the same membrane, followed by normalization with the 5S rRNA signal. To exclude a systematic effect of the inducers (IPTG and arabinose) on target RNA levels in the different strain backgrounds in presence of the *glmZ'-gfp* fusion, target RNA levels from this study were analyzed in their respective strain backgrounds. Each strain carried plasmids pYG205, for production of RapZ, and pYG215 for expression the *glmZ'-gfp* fusion RNA. IPTG (1 mM) and arabinose (0.2 %) were added in different combinations as indicated (- IPTG/- ara, + IPTG/- ara, - IPTG/+ ara, + IPTG/+ ara). The respective target RNAs were analyzed by Northern Blot and signal intensities were quantified. The resulting bar graphs present the average normalized target RNA signal intensities and SD for (A) *ompD* mRNA in strain Z1129, (B) *sodB* mRNA in Z1013, (C) *nhaB* mRNA in Z1012 and (D) *GcvB* sRNA in Z1014. Number of replicates (n) are indicated

under the respective bars. In each strain background RNA signal intensities under different inducer combinations were compared to the signal intensity obtained in the + IPTG/+ ara condition, which was set to 100 %, and normalized to the corresponding 5S rRNA loading controls.

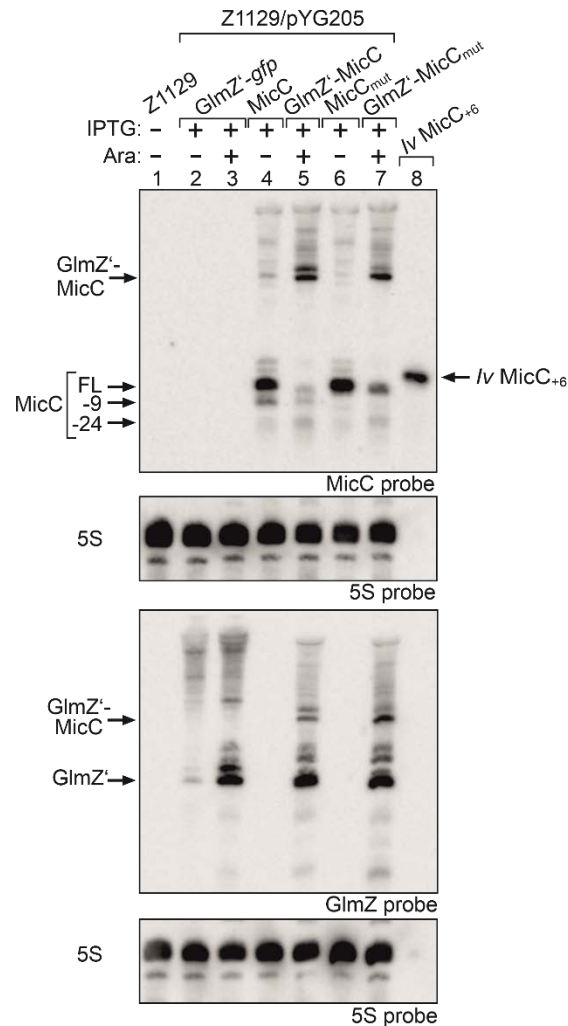
Supplementary Figure S2



Supplementary Figure S2. Increasing the distance between GlmZ' and the MicC start nucleotide in the *glmZ'*-*micC* fusion by one or two nucleotides has no impact on the regulatory performance of the released 5'P-MicC species. Northern blot experiment addressing *ompD* steady state levels in strains producing 5'PPP-MicC or various 5'P-MicC variants. Strain Z1129 ($\Delta micC \Delta glmY \Delta glmZ \Delta rapZ \lambda attB::P_{lac}-ompD$), containing plasmid pYG205, carried either control plasmid pYG215 (*glmZ'*-gfp, lanes 2-4), pYG314 (*micC*, lane 5), pYG313 (*glmZ'*-*micC*, lanes 6-8), pAS13 (*glmZ'*-*micC*_G, lanes 9-11) or plasmid pAS14 (*glmZ'*-*micC*_{GG}, lanes 12-14). The latter two plasmids carry *glmZ'*-*micC* fusion genes with one or two additional G residues inserted in front of the *micC* start nucleotide. The empty strain Z1129 was included as control (lane 1). 1 mM IPTG and 0.2% arabinose were added as indicated (“+”). Following growth, total RNAs were extracted and separated (1.5 μ g each) on 5% and 8% PAA gels, respectively, and subsequently blotted. The blot of the 5% PAA gel was consecutively hybridized with probes detecting *ompD* and GlmZ (first and second panel from top), whereas the

blot of the 8% gel was probed for MicC (forth panel from top). Blots were re-probed for 5S rRNA to obtain loading controls. MicC and its decay products are indicated with arrows.

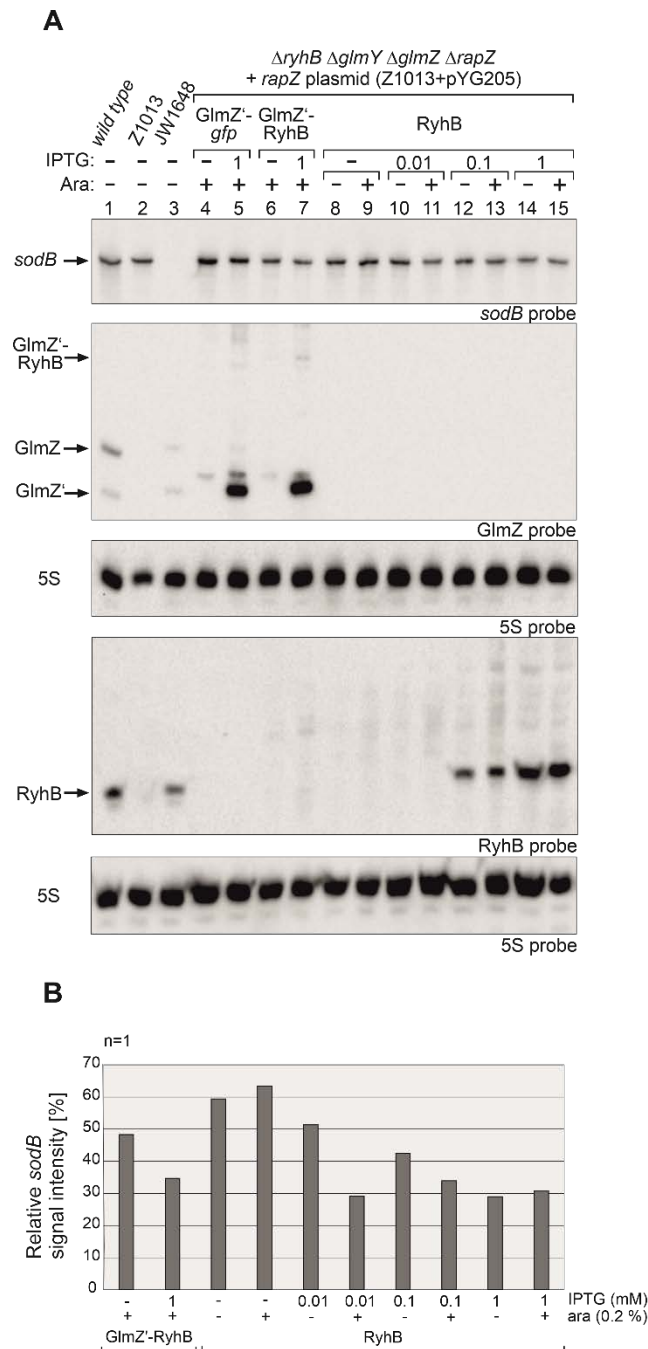
Supplementary Figure S3



Supplementary Figure S3. Mutation of the RNase E cleavage site at position +9 increases steady state levels of 5'P-MicC significantly. Northern blot experiment comparing steady state levels of wild-type MicC and the MicC_{mut} variant, carrying U₁₁U₁₂→C₁₁C₁₂ exchanges, abolishing RNase E cleavage at pos. +9. MicC and MicC_{mut} were either produced as 5'PPP-RNAs using plasmids pYG314 (lane 4) and pAS3 (lane 6) or in a 5'P state through release from the GlmZ' aptamer using plasmids pYG313 (lane 5) and pAS2 (lane 7). The transformant transcribing the *glmZ'-gfp* fusion from plasmid pYG215 was included in lane 2 & 3. The plasmids were tested in strain Z1129, which additionally contained plasmid pYG205 for synthesis of RapZ. The empty strain Z1129 was included in lane 1. 1 mM IPTG and 0.2% arabinose were added as indicated. Total RNAs were isolated and 1.5 μg each were separated on two denaturing 8% PAA gels, respectively. MicC generated by *in vitro* transcription was loaded as size marker in lane 8. Due to

T7 promoter design, 6 foreign nucleotides were added to the 5' end of MicC. The DNA template for *in vitro* transcription was generated by PCR using oligonucleotides BG1823/BG1824. The resulting blots were hybridized with probes for MicC or GlmZ, respectively, and re-probed to obtain 5S rRNA signals.

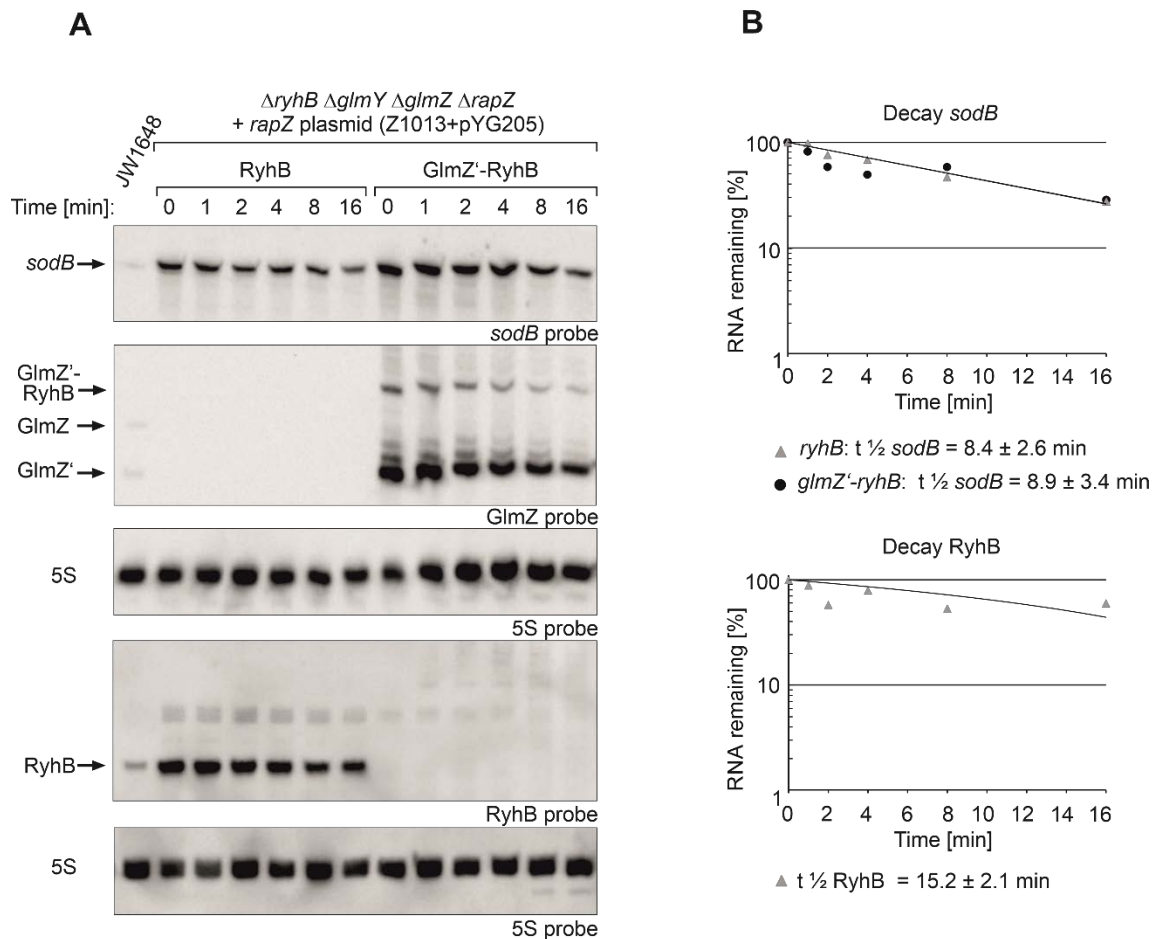
Supplementary Figure S4



Supplementary Figure S4. Comparison of the regulatory performance of 5’P- and 5’PPP-RyhB. (A) Similar experiment as shown in Figure 4, but as a difference various IPTG concentrations were used to induce transcription of 5’PPP-RyhB. The used strains and plasmid constructs are described in the legend of Figure 4. Total RNAs were isolated and separated (1.5 µg each; as exception 3 µg were loaded in lane 1) on two denaturing 5% PAA gels. After blotting,

one blot was consecutively hybridized with probes detecting *sodB* and GlmZ (first and second panel from top), while the other blot was probed for RyhB (fourth panel from top). Blots were re-probed for 5S rRNA to obtain loading controls. **(B)** Quantification of Northern blot. Bar graph presenting the normalized signal intensities of *sodB* (n=1). *sodB* mRNA signal intensities, in presence of RyhB and GlmZ-RyhB, were compared to *sodB* signal intensities obtained in presence of GlmZ'-*gfp* (lanes 4, 5; = 100 %) and normalized to the corresponding 5S rRNA loading controls.

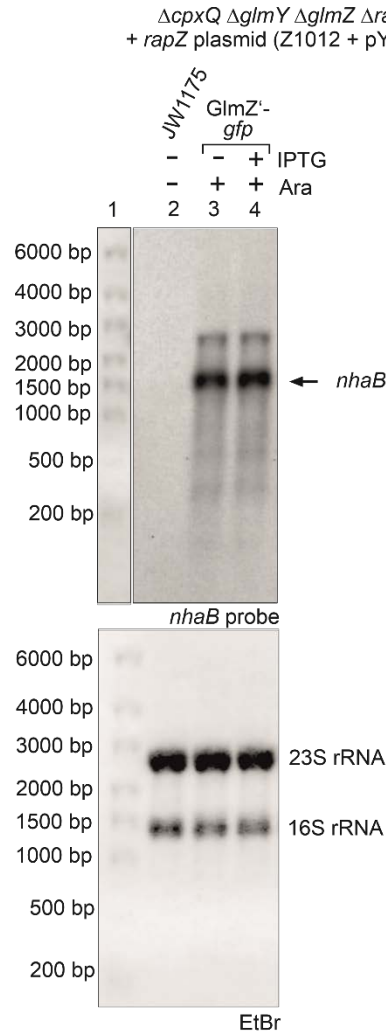
Supplementary Figure S5



Supplementary Figure S5. Determination of *sodB* decay rates triggered by 5'PPP- and 5'P-RyhB and analysis of RyhB stability. (A) Northern blot for determination of *sodB* decay rates in presence of 5'PPP-RyhB and 5'P-RyhB and evaluation of RyhB stability. Transcription was stopped with rifampicin (t_0) and samples were removed at indicated times for RNA extraction and Northern blotting. Strain Z1013 ($\Delta ryhB \Delta glmY \Delta glmZ \Delta rapZ$) carried plasmid pYG205 and additionally either plasmid pYG275 (*ryhB*) or plasmid pYG274 (*glmZ'-ryhB*). Strain JW1648 ($\Delta sodB$) was included in lane 1. The bacteria were grown in presence of 1 mM IPTG to induce transcription of *ryhB* and the *glmZ'* fusion genes. Arabinose (0.2 %) was added to trigger RapZ-mediated cleavage of the fusion RNAs. Total RNAs (1.5 μ g each) were separated on two denaturing PAA gels, containing 5% or 8% acrylamide, and subsequently blotted. The blot resulting from the 5% PAA gel was consecutively hybridized with probes detecting *sodB* and GlmZ (first and second panel from top), while the other blot was probed for RyhB (fourth panel from top). Blots were re-probed for 5S rRNA to obtain loading controls. (B) Semi-logarithmic plots of *sodB*

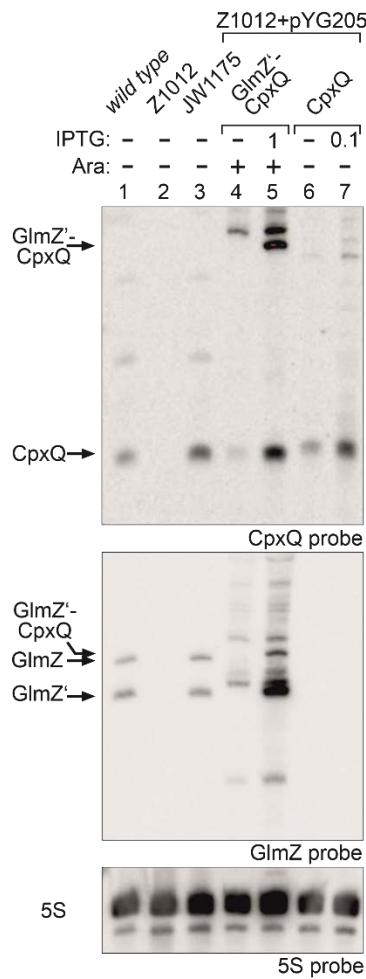
and RyhB signal intensities for half-life determination. The data are presented as mean, $n = 2$. Half-lives values are presented as mean \pm SD.

Supplementary Figure S6

**Supplementary Figure S6. Northern blot addressing the precise size of the *nhaB* mRNA.**

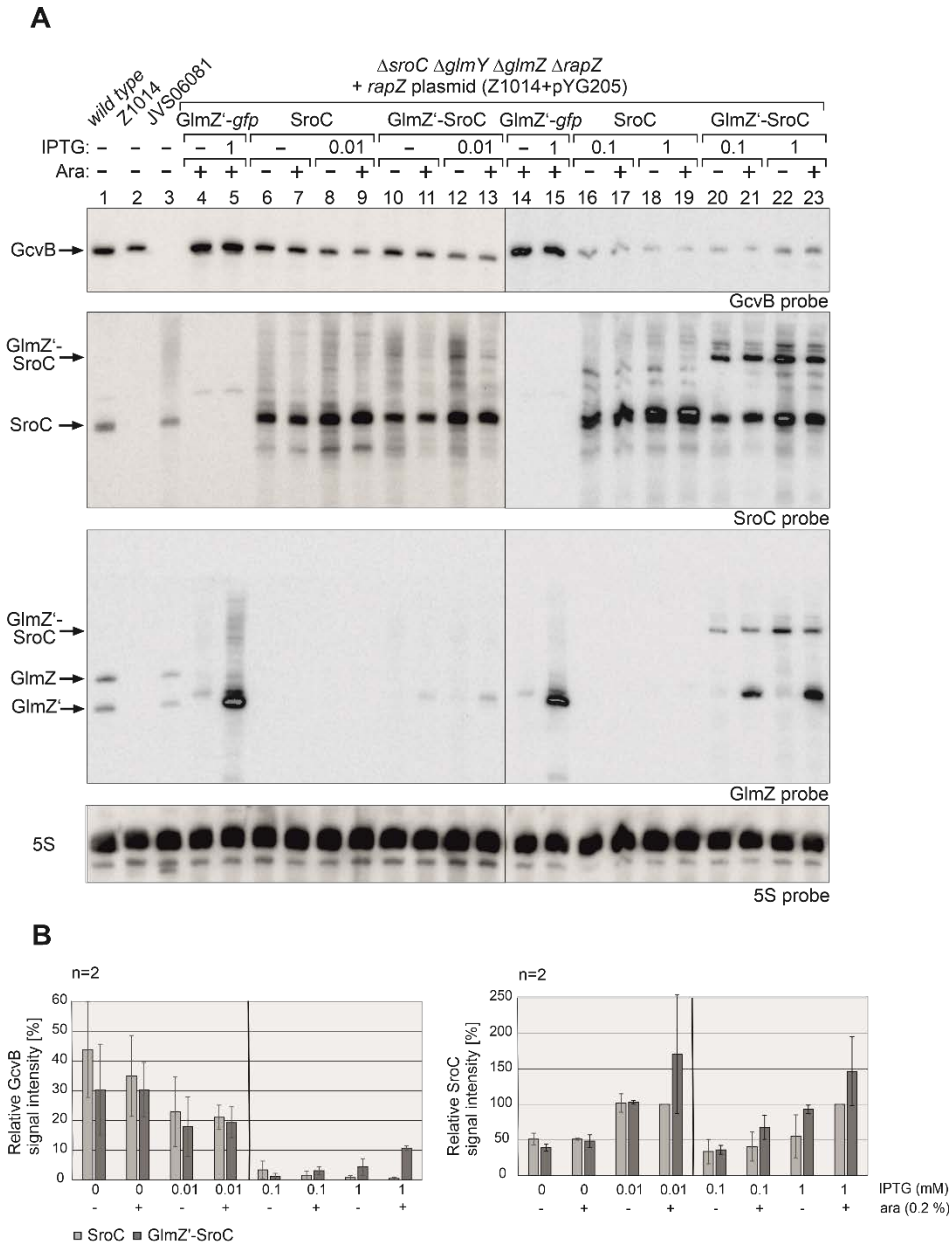
Total RNA extracted from strain Z1012 ($\Delta cpxQ \Delta glmY \Delta glmZ \Delta rapZ$) containing plasmids pYG205 (*rapZ*) and pYG215 (*glmZ'*-*gfp*, lanes 3, 4) was loaded next to an RNA size marker RiboRuler High Range RNA Ladder (Thermo Scientific; lane 1). Strain JW1175 ($\Delta nhaB$, lane 2) demonstrates *nhaB* probe specificity. IPTG (1 mM) and arabinose (0.2 %) was added as indicated. To detect *nhaB* mRNA (first panel from top), 3.5 μ g of total RNA was separated on an 1 % agarose gel and subsequently transferred to the membrane via vacuum blotting. EtBr stained 23S/16S rRNAs and the RNA ladder were visualized after blotting in a ChemiDoc (second panel from top).

Supplementary Figure S7



Supplementary Figure S7. Comparison of gel migration velocities of 5'PPP-CpxQ and CpxQ derived from the GlmZ'-CpxQ fusion with endogenous CpxQ. Northern blot addressing size differences between CpxQ variants. Total RNAs extracted from the empty strains S4197 (*wild-type*), Z1012 ($\Delta cpxQ$, $\Delta glmY$ $\Delta glmZ$ $\Delta rapZ$), and JW1175 ($\Delta nhaB$) were analyzed in lanes 1-3. RNAs (3 μ g in lanes 1-3; 1.5 μ g in lanes 4-7) were separated on an 8% denaturing PAA gel, blotted and consecutively hybridized with probes detecting CpxQ, GlmZ and 5S rRNA.

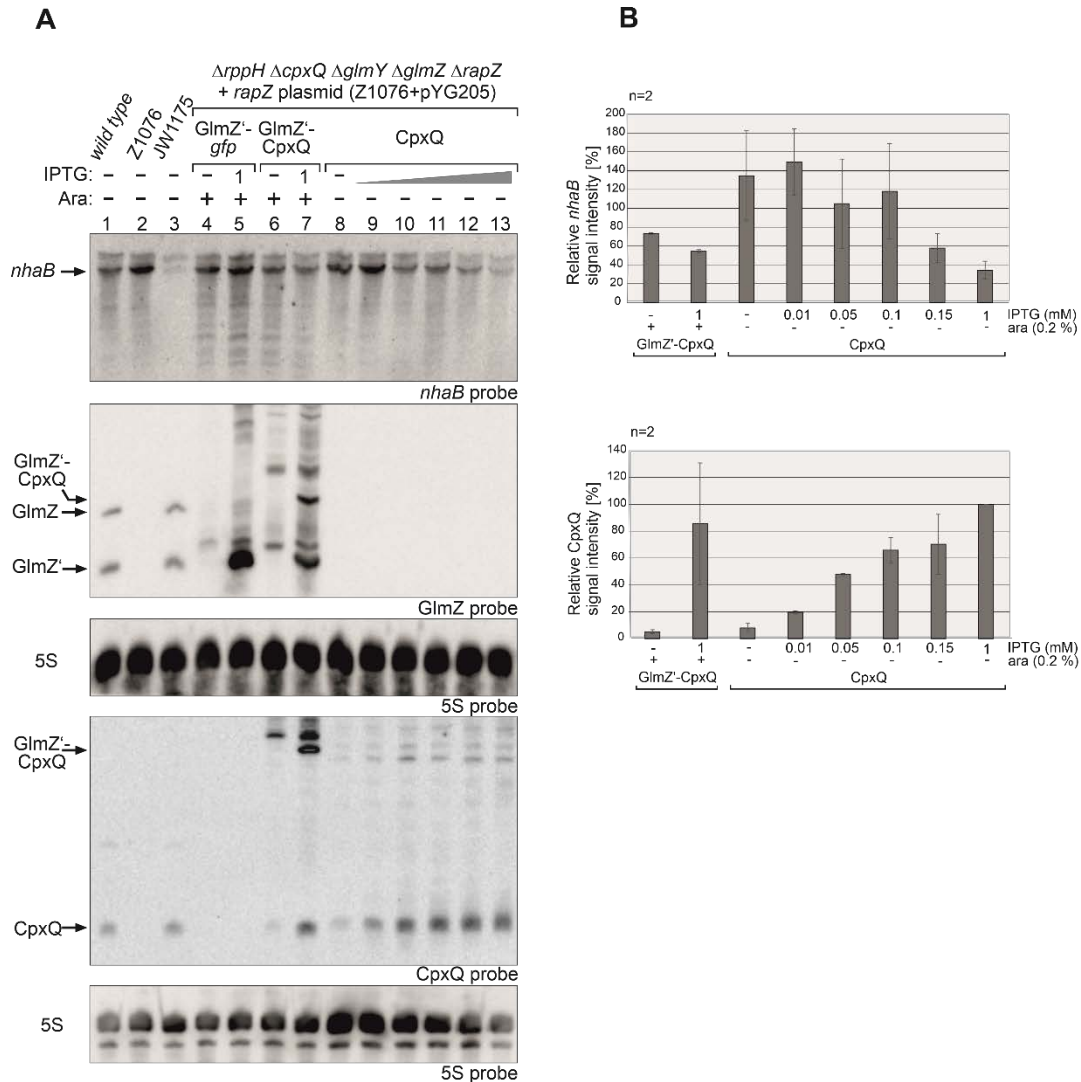
Supplementary Figure S8



Supplementary Figure S8. Analysis of GcvB repression by 5'PPP- and 5'P-SroC. (A) Northern blot experiment addressing GcvB steady state levels in presence of the GlmZ'-*gfp* control fusion, 5'PPP-SroC and 5'P-SroC. Strain Z1014 ($\Delta sroC \Delta glmY \Delta glmZ \Delta rapZ$) carried plasmid pYG205 (*rapZ*) and additionally either plasmid pYG215 (*glmZ'-gfp*, lanes 4, 5, 14, 15), pYG277 (*sroC*, lanes 6-9 and 16-19) or plasmid pYG276 (*glmZ'-sroC*, lanes 10-13 and 20-23). The empty strains S4197 (*wild-type*), Z1014 ($\Delta sroC, \Delta glmY \Delta glmZ \Delta rapZ$), and JVS06081 ($\Delta gcvB$) were

included to demonstrate specificity of probes (lanes 1-3). Bacteria were grown in absence or presence of arabinose and various concentrations of IPTG as indicated. Total RNAs (1.5 μ g each, as exception 3 μ g were loaded in lane 1) were separated on two denaturing 8% PAA gels and subsequently blotted. The blots were consecutively hybridized with probes detecting GcvB, SroC, GlmZ and 5S rRNA. **(B)** Quantification of Northern blots. Bar graphs presenting the average normalized signal intensities and SD of 2 independent experiments. GcvB signal intensities, in presence of SroC (light grey) and GlmZ'-SroC (dark grey), were compared to GcvB signal intensities obtained in presence of GlmZ'-*gfp* on the respective membrane (lanes 4, 5 or 14, 15; = 100 %) and normalized to the corresponding 5S rRNA loading controls (left graph). SroC signal intensities (SroC, light grey; GlmZ'-SroC, dark grey) were compared to the signal intensity obtained for SroC in lane 9 (=100 %) or lane 19 (=100 %) on the respective membrane and normalized to the 5S rRNA loading controls (right graph).

Supplementary Figure S9

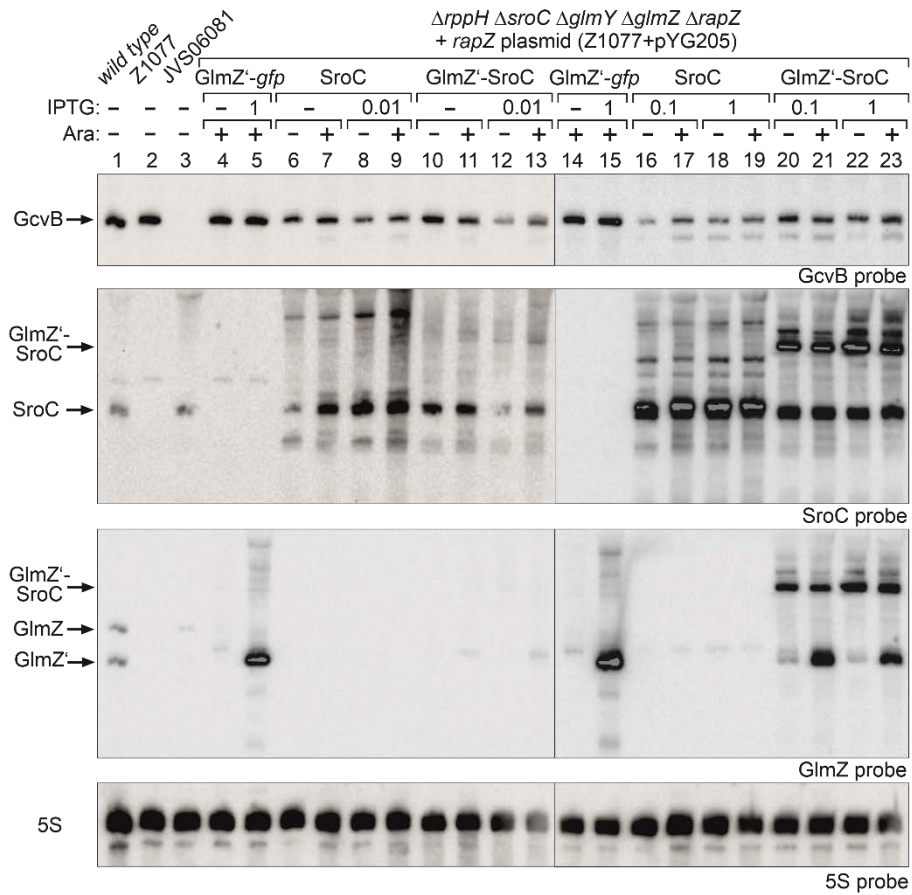


Supplementary Figure S9. Comparison of the regulatory strength of 5'P- and 5'PPP-CpxQ in a strain lacking pyrophosphohydrolase RppH. (A) Similar experiment as shown in Figure 5, but as a difference strain Z1076, additionally lacking the *rppH* gene, was used for comparison of *nhaB* mRNA levels in presence of 5'PPP-CpxQ or 5'P-CpxQ. The empty strains S4197 (*wild-type*), Z1076 ($\Delta rppH \Delta cpxQ, \Delta glmY \Delta glmZ \Delta rapZ$), and JW1175 ($\Delta nhaB$) were included in lanes 1-3. Total RNAs were isolated and 1.5 μ g of each sample was separated on two denaturing PAA gels containing 5% and 8% acrylamide, respectively. Resulting blots were consecutively hybridized with probes detecting *nhaB* (first panel from top) and GlmZ (second panel from top) or probed for CpxQ (fourth panel from top). Both membranes were re-probed for 5S rRNA to obtain loading controls. (B) Quantification of Northern blots. Bar graphs presenting the average normalized signal

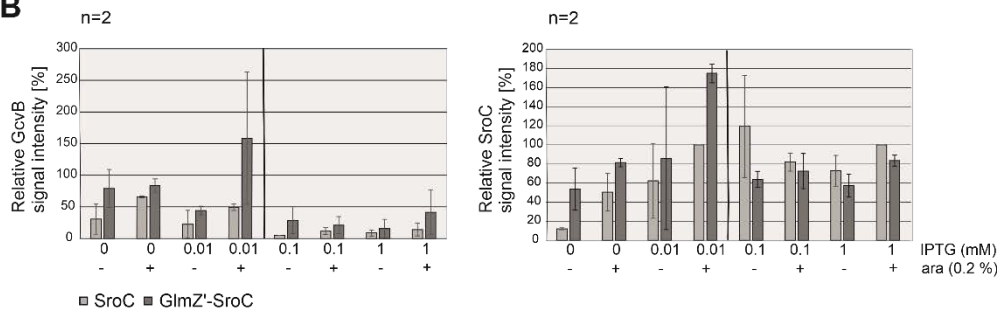
intensities and SD of 2 independent experiments. *nhaB* mRNA signal intensities, in presence of GlmZ'-CpxQ and CpxQ, were compared to *nhaB* signal intensities obtained in presence of GlmZ'-*gfp* (lanes 4, 5; = 100 %) and normalized to the corresponding 5S rRNA loading controls (top graph). CpxQ signal intensities were compared to the strongest signal obtained for CpxQ (lane 13; = 100 %) and normalized to the 5S rRNA loading controls (bottom graph).

Supplementary Figure S10

A



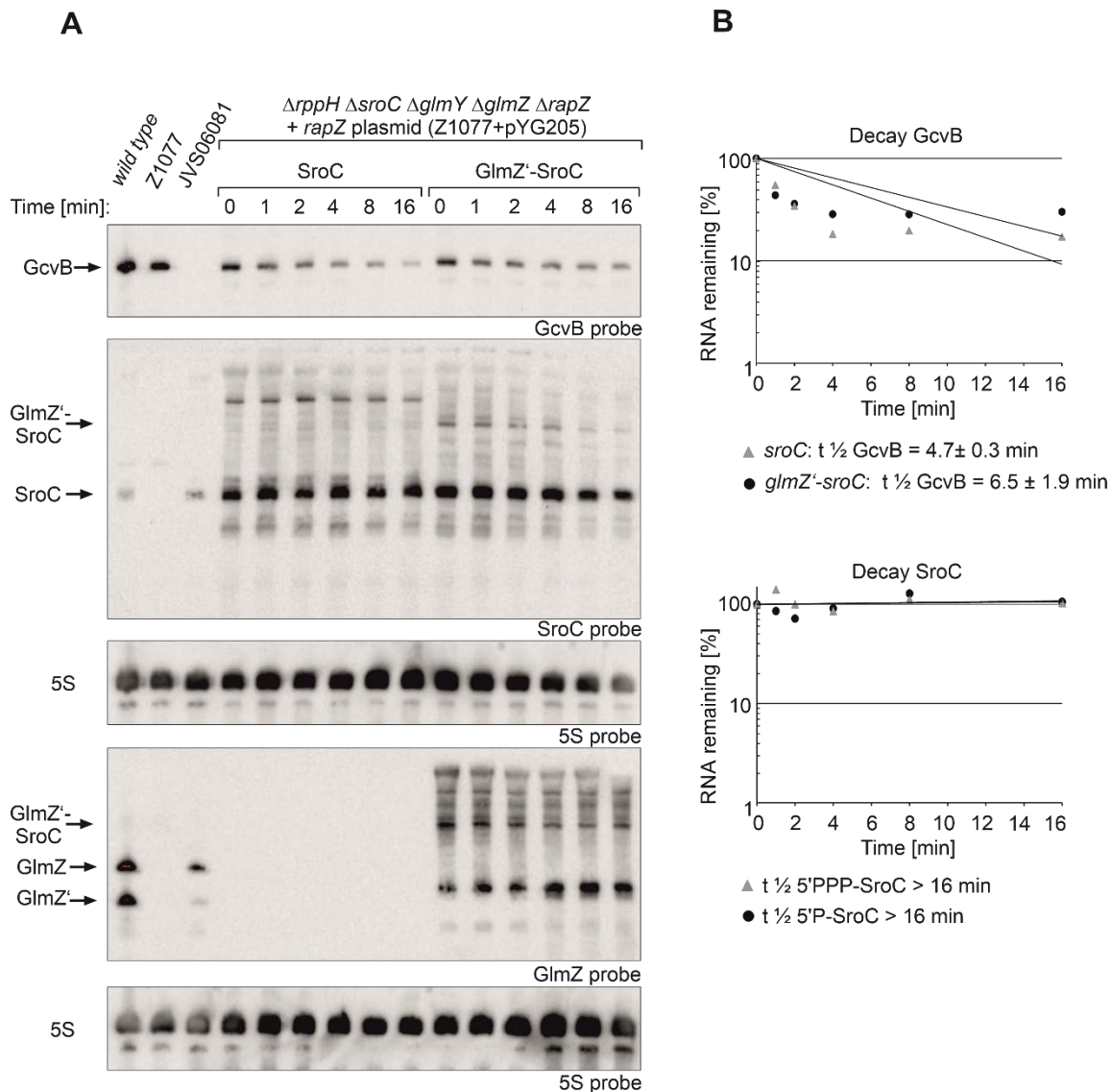
B



Supplementary Figure S10. Comparison of the regulatory strength of 5'PPP- and 5'P-SroC in a strain lacking pyrophosphohydrolase RppH. (A) Similar experiment as shown in Supplementary Figure S8, but strain Z1077, lacking additionally the *rppH* gene, was used for comparison of GcvB levels in presence of 5'PPP- SroC or 5'P-SroC. Bacteria were grown in absence or presence of arabinose and various concentrations of IPTG as indicated. Total RNAs (1.5 μ g each; as exception 3 μ g were loaded in lane 1) were separated on two denaturing 8% PAA

gels and subsequently blotted. The blots were consecutively hybridized with probes detecting GcvB, SroC, GlmZ and 5S rRNA. **(B)** Quantification of Northern blots. Bar graphs presenting the average normalized signal intensities and SD of 2 independent experiments. GcvB signal intensities, in presence of SroC (light grey) and GlmZ'-SroC (dark grey), were compared to GcvB signal intensities obtained in presence of GlmZ'-*gfp* on the respective membrane (lanes 4, 5 or 14, 15; = 100 %) and normalized to the corresponding 5S rRNA loading controls (left graph). SroC signal intensities (SroC, light grey; GlmZ'-SroC, dark grey) were compared to the signal intensity obtained for SroC in lane 9 (=100 %) or lane 19 (=100 %) on the respective membrane and normalized to the 5S rRNA loading controls (right graph).

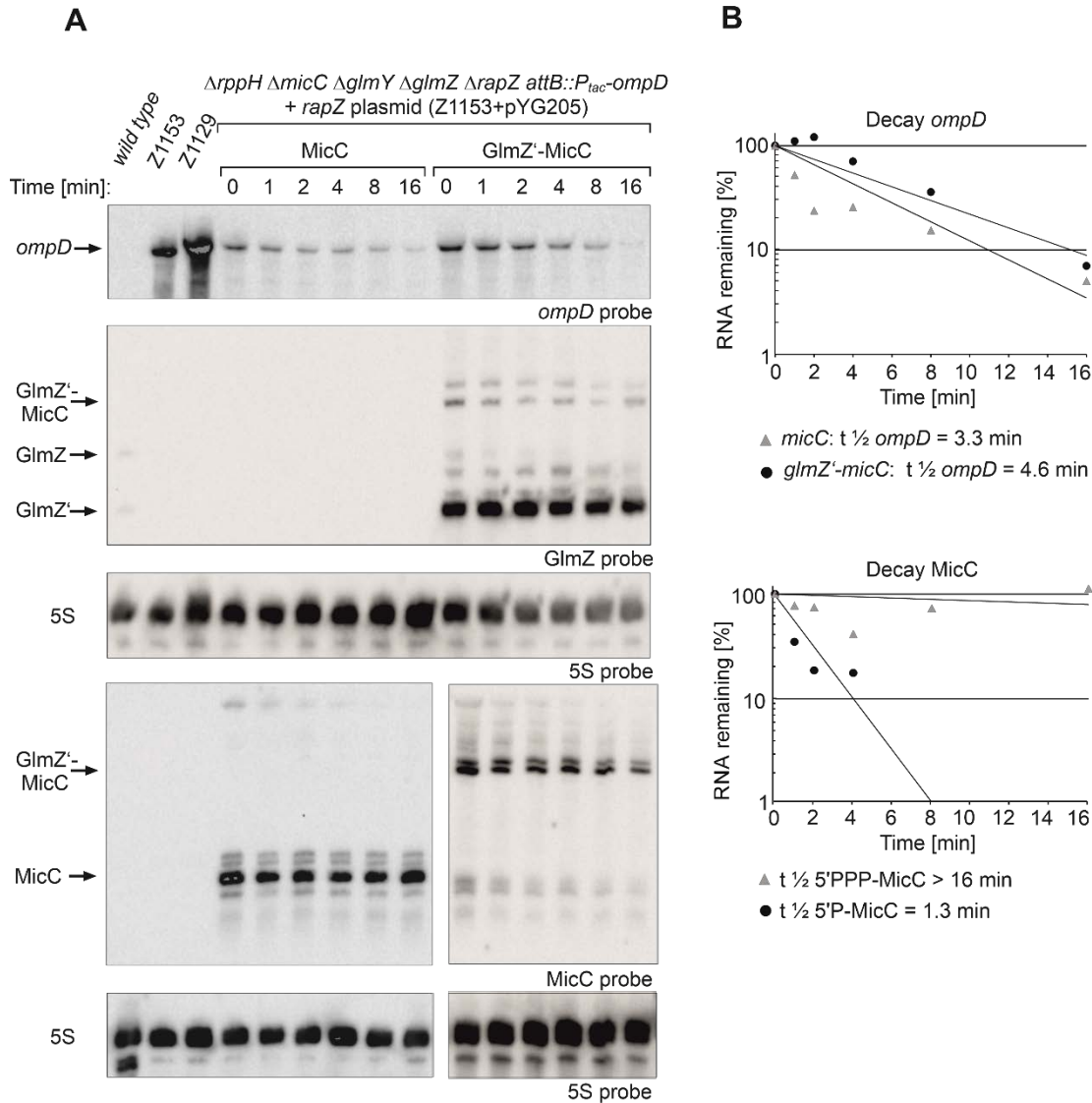
Supplementary Figure S11



Supplementary Figure S11. Comparison of GcvB decay rates triggered by 5'PPP- and 5'P-SroC in a strain lacking pyrophosphohydrolase RppH. (A) Similar experiment as shown in Figure 7, but as a difference the $\Delta rppH$ strain Z1077 was used for comparison of GcvB decay in presence of 5'PPP-SroC or 5'P-SroC and analysis of SroC stability. The transformants were grown in presence of 0.01 mM IPTG to induce transcription of *sroC* and the *glmZ'* fusion genes. Arabinose (0.2%) was additionally added to trigger cleavage of the fusion RNAs. Total RNAs were isolated and separated (1.5 μ g each; as exception 3 μ g were loaded in lane 1) on two denaturing 8% PAA gels, respectively. After blotting, one blot was consecutively hybridized with probes detecting GcvB and SroC (first and second panel from top), while the other blot was probed for GlmZ (fourth panel from top). Blots were re-probed for 5S rRNA to obtain loading controls. **(B)**

Semi-logarithmic plots of GcvB and SroC signal intensities for half-life determination. The data are presented as mean, $n = 2$. Half-lives values are presented as mean \pm SD.

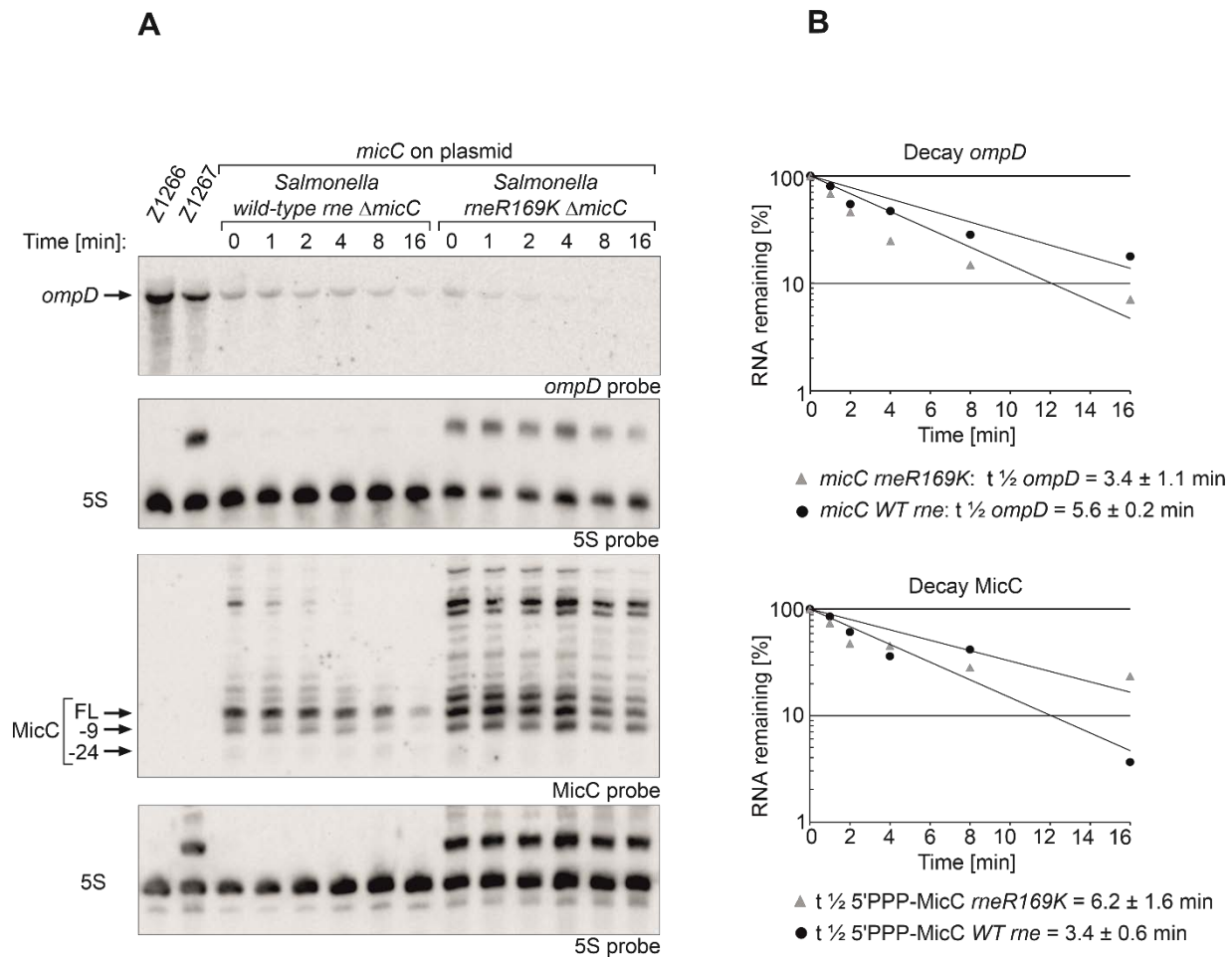
Supplementary Figure S12



Supplementary Figure S12. Comparison of *ompD* decay rates triggered by 5'PPP- and 5'P-MicC in a strain lacking pyrophosphohydrolase RppH. (A) Similar experiment as shown in Figure 3, but as a difference the isogenic $\Delta rppH$ strain Z1153 was used for comparison of *ompD* decay in presence of 5'PPP-MicC or 5'P-MicC and determination of MicC stability. The transformants were grown in presence of 1 mM IPTG to induce transcription of *micC* and the *glmZ'* fusion genes. Arabinose (0.2 %) was added to trigger cleavage of the fusion RNAs. Total RNAs (1.5 μ g each) were separated on two denaturing PAA gels containing 5% or 8% acrylamide, respectively, and subsequently blotted. The blot resulting from the 5% PAA gel was consecutively hybridized with probes detecting *ompD* and GlmZ (first and second panel from top), while the other blot was probed for MicC (fourth panel from top). Blots were re-probed for 5S rRNA to obtain

loading controls. **(B)** Semi-logarithmic plots of *ompD* and MicC signal intensities for half-life determination of one experiment (n=1).

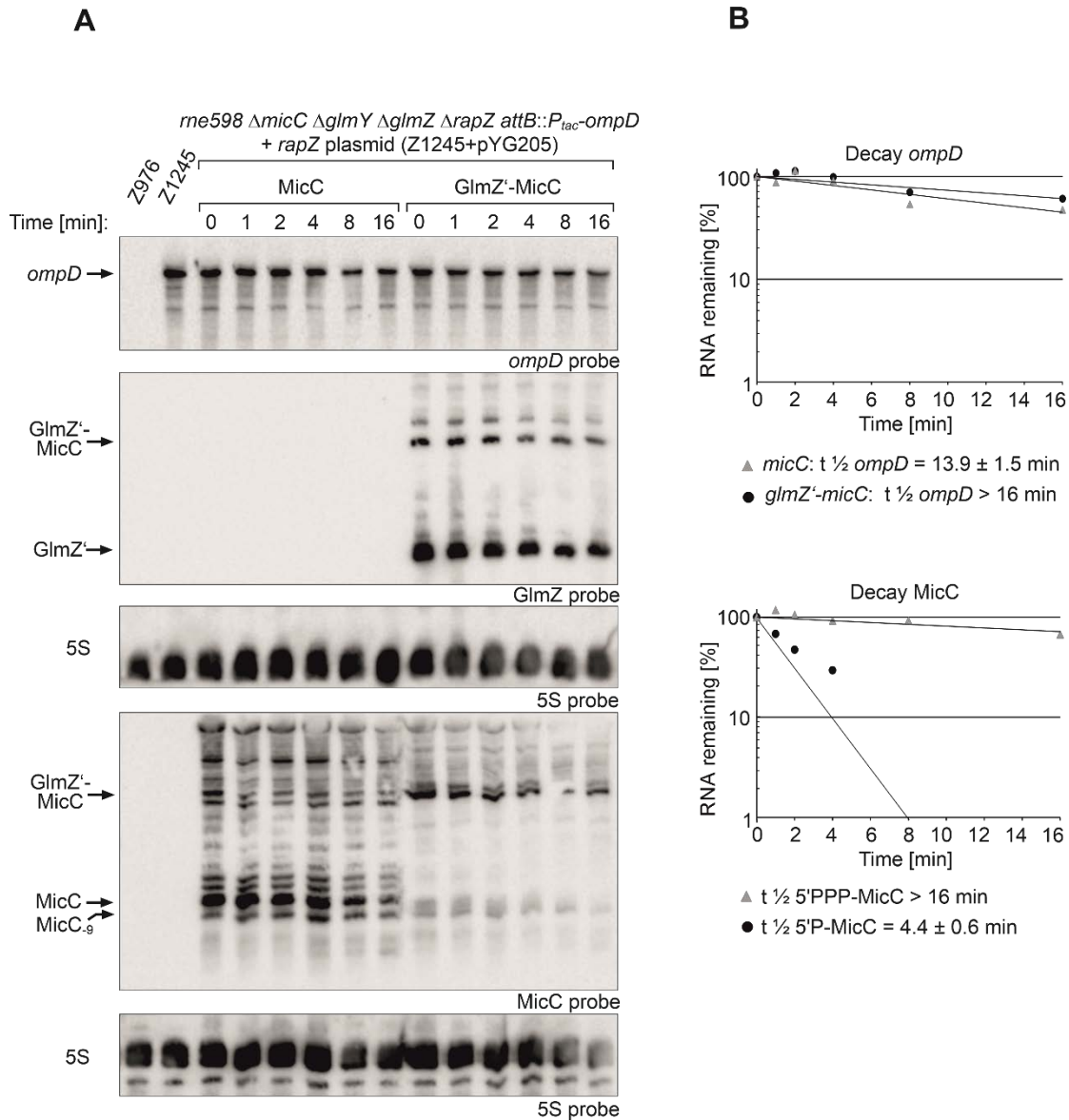
Supplementary Figure S13



Supplementary Figure S13. Analysis of *ompD* decay triggered by MicC in *Salmonella* strains synthesizing wild-type RNase E or the RNase E R169K variant. (A) Northern blots showing *ompD* mRNA and 5'PPP-MicC decay in *Salmonella Typhimurium* strains Z1266 (WT *rne*, $\Delta micC$) and Z1267 (*rneR169K*, $\Delta micC$), respectively. Bacterial strains were transformed with plasmid pYG314 transcribing MicC from the $P_{LlacO-1}$ promoter. The empty strains Z1266 and Z1267 were included in lane 1 and 2. The transformants were grown in presence of 1 mM IPTG to induce transcription of *micC*. Transcription was stopped with rifampicin (t_0) and samples were harvested at indicated times for RNA extraction and Northern blotting. Total RNAs (1.5 μg each) were separated on two denaturing PAA gels, containing 5% and 8% acrylamide, and were subsequently blotted. Membranes were hybridized with the respective probes to detect *ompD* (top panel) and MicC (third panel). Blots were re-probed for 5S rRNA to obtain loading controls. Full-length (FL) MicC and its decay products are indicated with arrows. (B) Semi-logarithmic plots of *ompD* and MicC signal intensities for half-life determination. The data are presented as mean, $n = 2$. Half-

lives values are presented as mean \pm SD. In the *rneR169K* strain, signal intensities of the 5S signal and the 5S rRNA precursor were summed up for normalization.

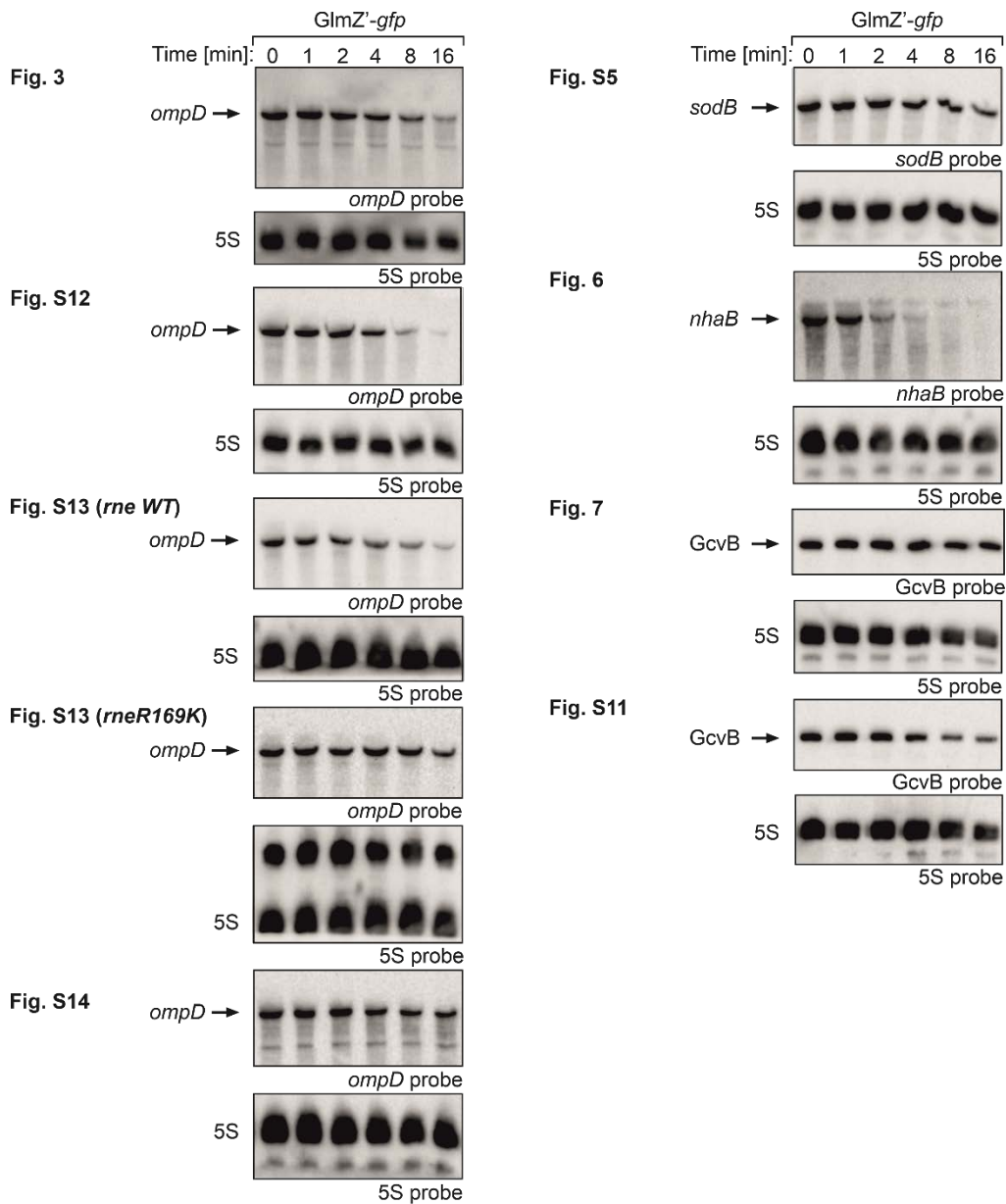
Supplementary Figure S14



Supplementary Figure S14. Determination of *ompD* decay rates triggered by 5'PPP- and 5'P-MicC in a strain expressing the truncated *rne598* variant. (A) Similar experiment as shown in Figure 3, but as a difference the *rne598* strain Z1245 was used. The transformants were grown in presence of 1 mM IPTG to induce transcription of *micC* and the *glmZ'* fusion genes. Arabinose (0.2 %) was added to trigger RapZ-mediated cleavage of the fusion RNAs. Total RNAs were extracted and separated (1.5 μ g each) on two denaturing PAA gels, containing 5% or 8% acrylamide, respectively. After blotting, the membrane resulting from the 5% PAA gel was consecutively hybridized with probes detecting *ompD* and GlmZ (first and second panel from top), while the other blot was probed for MicC (fourth panel from top). Blots were re-probed for 5S rRNA

to obtain loading controls. **(B)** Semi-logarithmic plots of *ompD* and MicC signal intensities for half-life determination. The data are presented as mean, n = 2. Half-lives values are presented as mean \pm SD.

Supplementary Figure S15



Supplementary Figure S15. RNA half-life experiments in presence of the *GlmZ'-gfp* fusion RNA to show sRNA-specific target destabilization. For each strain background, as listed in Table 1, control experiments in absence of the respective sRNA were performed. Thus, strains expressing the *glmZ'-gfp* (pYG215) fusion were grown in parallel and treated the same as the cultures expressing the respective sRNA variants. One representative Northern blot for each strain background is shown. Target RNA half-lives were calculated as described from 1-3 independent experiments.

SUPPLEMENTARY MATERIALS AND METHODS

Construction of plasmids

Plasmid pYG205 was obtained by replacing the *Sall-XbaI* fragment comprising *strep-rapZ* in plasmid pYG13 with a PCR fragment obtained with oligonucleotides BG1307/BG397 and plasmid pFDX4324 as template. This construction places *wild-type rapZ* provided with the RBS of the *Bacillus subtilis sacB* gene under P_{Ara} control. Plasmid pYG215 was constructed in several steps. First, the *XhoI-NdeI* fragment comprising the operator-less P_{tac} and the *ptsN* gene in the pSC101 derivative plasmid pFDX4294 was replaced with a PCR fragment carrying the *lacI^q* allele. The latter fragment was generated using primers BG1316/BG1337 and plasmid pKES170 as template. In the resulting plasmid pYG192, a novel *PstI* site was introduced by reverse primer BG1337. Next, a PCR fragment comprising the $P_{LacO1}::glmZ'-rpsT-3xFLAG \lambda_{t0} tet$ cassette from plasmid pYG183 was amplified using primers BG1318/BG1319 and cloned between the *AgeI-PstI* sites on plasmid pYG192, resulting in plasmid pYG193. Finally, the *gfpmut3** gene was amplified with BG1345/BG1354 from plasmid pYG213 and used to replace the *AgeI-XbaI* fragment comprising *rpsT-3xFLAG* in plasmid pYG193, resulting in plasmid pYG215.

Plasmid pYG315 carries the *Salmonella ompD* gene (-69 to +1178) under control of an operator-less P_{tac} promoter and allows for site-specific integration of the latter cassette into the $\lambda attB$ site on the *E. coli* chromosome. Its construction, which involved several intermediate steps, is based on plasmid pKEM20, which is designed for integration of translational *lacZ* fusions into the *E. coli* $\lambda attB$ site. First, the *Sall-XbaI* fragment comprising *proV'* in pKEM20 was replaced with a *glmS'* (-311 to +129) fragment, which created a translational *glmS'-lacZ* fusion on the resulting plasmid pBGG19. The *glmS'* fragment was generated by PCR using primers BG121/BG123. Subsequently, the *XbaI-TatI* fragment comprising the *lacZ* gene was replaced with the sequence encoding superfolder (sf) GFP (including its RBS). The *sf-gfp* fragment was amplified using primers BG1456/BG1455 and plasmid pXG10-SF (1) as template and digested with *XbaI* and *Acc65I* prior to ligation with the *TatI-XbaI* vector backbone of plasmid pBGG19. This construction created a transcriptional *glmS'-sf-gfp* fusion on the resulting plasmid pMK5 and introduced a novel *PstI* site downstream of the sf-gfp CDS. Next, the *PvuII-XbaI* fragment comprising the *glmS* 5' region was replaced with a PCR fragment obtained by using oligonucleotides BG1457/BG123 and plasmid pMK5 as template. The forward primer BG1457 introduced the sequence of an operator-less P_{tac} promoter upstream of *glmS'*, resulting in plasmid pMK7. Finally, the *Sall-PstI* fragment encompassing the $P_{tac}::glmS'-sf-gfp$ fusion in pMK7 was replaced with a PCR fragment generated with primers BG1705/BG1720 using chromosomal DNA of *Salmonella Typhimurium* SL1344 as

template. Forward primer BG1705 anneals to the *ompD* 5' UTR and reintroduces the operator-less P_{tac} promoter, thereby creating the $P_{tac}::ompD$ fusion in plasmid pYG315.

The plasmids transcribing the various *glmZ'*-sRNA fusion RNAs from P_{LacO-1} were obtained by replacing the *AgeI-XbaI* fragment in plasmid pYG215 with PCR fragments comprising the sRNA sequence of choice. The latter were amplified using chromosomal DNAs of *E. coli*-K12 (*ryhB*, *cpxQ*, *sroC*) or *Salmonella Typhimurium* SL1344 (*micC*) as templates and the following oligonucleotides resulting in the mentioned plasmids: *glmZ'*-*cpxQ* (BG1493+BG1514, pYG272); *glmZ'*-*micC* (BG1700+BG1702, pYG313); *glmZ'*-*micC_G* (BG2045+BG1702; pAS13); *glmZ'*-*micC_{GG}* (BG2046+BG1702; pAS14); *glmZ'*-*micC_{mut}* (BG1797+BG1702; pAS2); *glmZ'*-*ryhB* (BG1489+BG1513; pYG274); *glmZ'*-*sroC* (BG1497+BG1515; pYG276).

The plasmids transcribing the sRNAs as primary transcripts from P_{LacO-1} were generated by substitution of the *AatII-XbaI* fragment in plasmid pYG215 with the sRNA sequences of choice. The various sRNAs were amplified from chromosomal DNA using the following oligonucleotides resulting in mentioned plasmids: *cpxQ* (BG1496+BG1514, pYG273), *micC* (BG1701+BG1702, pYG314); *micC_{mut}* (BG1798+B1702, pAS3); *ryhB* (BG1492+BG1513; pYG275); *sroC* (BG1500+BG1515; pYG277).

SUPPLEMENTARY TABLES

Supplementary Table I. Bacterial strains used in this study.

Name	Genotype	Reference
<i>Escherichia coli</i> -K12		
JVS06081	TOP10 Δ gcvB::kan	(2)
JVS8024	MC4100 Δ glmZ::kan	(3)
JW1175	<i>F</i> Δ (araD-araB)567 Δ lacZ4787(::rmB-3) λ : Δ haB::kan rph-1 Δ (rhaD-rhaB)568, hsdR514	(4)
JW1648	<i>F</i> Δ (araD-araB)567 Δ lacZ4787(::rmB-3) λ : Δ sodB::kan rph-1 Δ (rhaD-rhaB)568, hsdR514	(4)
JW2798	<i>F</i> Δ (araD-araB)567 Δ lacZ4787(::rmB-3) λ : Δ rppH754::kan rph-1 Δ (rhaD-rhaB)568, hsdR514	(4)
S4197	MG1655 rph* iivG* Δ lacZ	(5)
TM529	W3110 mic rne598-FLAG-cat	(6)
Z24	CSH50 Δ (pho-bgl)201 Δ (lac-pro) ara thi Δ rapZ::cat	(7)
Z95	CSH50 Δ (pho-bgl)201 Δ (lac-pro) ara thi Δ glmY::cat	(8)
Z836	S4197 Δ rapZ::cat	T4GT7 (Z24) \rightarrow S4197; this work
Z840	S4197 Δ rapZ	Z836 cured from cat; this work
Z933	S4197 Δ glmY::cat Δ rapZ	T4GT7 (Z95) \rightarrow Z840; this work
Z953	S4197 Δ glmY::cat Δ glmZ::kan Δ rapZ	T4GT7 (JVS8024) \rightarrow Z933; this work
Z956	S4197 Δ glmY Δ glmZ Δ rapZ	Z953 cured from cat and kan; this work
Z975	S4197 Δ micC::cat Δ glmY Δ glmZ Δ rapZ	PCR BG1399+BG1400 \rightarrow Z956, this work
Z976	S4197 Δ micC Δ glmY Δ glmZ Δ rapZ	Z975 cured from cat; this work
Z1012	S4197 Δ cpxQ::kan Δ glmY Δ glmZ Δ rapZ	PCR BG1503+BG1504 \rightarrow Z956, this work
Z1013	S4197 Δ ryhB::kan Δ glmY Δ glmZ Δ rapZ	PCR BG1501+BG1502 \rightarrow Z956, this work
Z1014	S4197 Δ sroC::kan Δ glmY Δ glmZ Δ rapZ	PCR BG1505+BG1506 \rightarrow Z956, this work
Z1047	S4197 Δ sroC Δ glmY Δ glmZ Δ rapZ	Z1014 cured from kan; this work
Z1048	S4197 Δ rppH::kan Δ sroC Δ glmY Δ glmZ Δ rapZ	T4GT7 (JW2798) \rightarrow Z1047; this work
Z1049	S4197 Δ cpxQ Δ glmY Δ glmZ Δ rapZ	Z1012 cured from kan; this work
Z1060	S4197 Δ cpxQ Δ glmY Δ glmZ Δ rapZ skip-3xFLAG::kan	PCR BG1615+BG1616 \rightarrow Z1049, this work
Z1061	S4197 Δ cpxQ Δ glmY Δ glmZ Δ rapZ skip-3xFLAG	Z1060 cured from kan; this work
Z1062	S4197 Δ rppH::kan Δ cpxQ Δ glmY Δ glmZ Δ rapZ skip-3xFLAG	T4GT7 (JW2798) \rightarrow Z1061; this work
Z1076	S4197 Δ rppH Δ cpxQ Δ glmY Δ glmZ Δ rapZ skip-3xFLAG	Z1062 cured from kan; this work
Z1077	S4197 Δ rppH Δ sroC Δ glmY Δ glmZ Δ rapZ	Z1048 cured from kan; this work
Z1129	S4197 Δ micC Δ glmY Δ glmZ Δ rapZ λ .attB::[operator-less P_{lac} ::ompD, aadA]	pYG315/BamHI \rightarrow Z976; this work
Z1152	S4197 Δ rppH::kan Δ micC Δ glmY Δ glmZ Δ rapZ λ .attB::[operator-less P_{lac} ::ompD, aadA]	T4GT7 (JW2798) \rightarrow Z1129; this work
Z1153	S4197 Δ rppH Δ micC Δ glmY Δ glmZ Δ rapZ λ .attB::[operator-less P_{lac} ::ompD, aadA]	Z1152 cured from kan; this work
Z1245	S4197 Δ micC Δ glmY Δ glmZ Δ rapZ rne598-FLAG-cat λ .attB::[operator-less P_{lac} ::ompD, aadA]	T4GT7 (TM529) \rightarrow Z1129; this work
<i>Salmonella enterica</i> serovar Typhimurium		
JVS6999	SL1344 (rluC-me)::Cm ^R me _{wt}	(9)
JVS10999	SL1344 (rluC-me)::Cm ^R meR169K	(9)
SL1344	Str ^R hisG rpsL xyl	(10)
Z1266	SL1344 (rluC-me)::Cm ^R micC::kan	PCR BG1973+BG1974 \rightarrow JVS6999, this work
Z1267	SL1344 (rluC-me)::Cm ^R meR169K micC::kan	PCR BG1973+BG1974 \rightarrow JVS10999, this work

Supplementary Table II. Plasmids used in this study.

Name	Relevant structure	Reference
pAS2	<i>lacI^q P_{LacO-1}::glmZ'-micC_{mut} λt₀ tet cat ori-pSC101</i> (<i>micC</i> mutated at pos.11/12: TT→CC)	this work
pAS3	<i>lacI^q P_{LacO-1}::micC_{mut} λt₀ tet cat ori-pSC101</i> (<i>micC</i> mutated at pos.11/12: TT→CC)	this work
pAS13	as pYG313, but additional G in front of <i>micC</i> start nucleotide	this work
pAS14	as pYG313, but two additional G (GG) in front of <i>micC</i> start nucleotide	this work
pBGG19	translational <i>glmS'</i> (-311 to +129)- <i>lacZ</i> fusion in pKEM20	this work
pFDX4291	operator-less <i>P_{lac} sacB-RBS MCS cat ori-pSC101</i>	(7)
pFDX4294	<i>ptsN</i> in pFDX4291	(7)
pFDX4324	<i>rapZ</i> in pFDX4291	(7)
pKEM20	<i>λattP aadA proV'-lacZ</i> (translational fusion, <i>proV'</i> substitutable via Sall/XbaI) <i>neo ori-p15A</i>	(11)
pKES170	<i>lacI^q P_{lac} RBS-T7gene10 MCS bla ori-ColEI</i>	(12)
pMK5	<i>λattP aadA glmS'-sf-gfp</i> (transcriptional fusion) <i>neo ori-p15A</i>	this work
pMK7	<i>λattP aadA</i> operator-less <i>P_{lac}::glmS'-sf-gfp</i> (transcriptional fusion) <i>neo ori-p15A</i>	this work
pYG13	<i>P_{Ara}::strep-rapZ</i> with <i>rapZ</i> RBS <i>araC λattP cat bla ori-ColEI</i>	(13)
pYG183	<i>P_{LacO-1}::glmZ'-rpsT-3xFLAG λt₀</i> in pBR-plac	(14)
pYG192	<i>lacI^q cat ori-pSC101</i>	this work
pYG193	<i>lacI^q P_{LacO-1}::glmZ'-rpsT-3xFLAG λt₀ tet cat ori-pSC101</i>	this work
pYG205	<i>P_{Ara}::rapZ</i> with <i>sacB</i> RBS <i>araC λattP cat bla ori-ColEI</i>	this work
pYG213	<i>P_{LacO-1}::glmZ'-gfpmut3* λt₀</i> in pBR-plac	(14)
pYG215	<i>lacI^q P_{LacO-1}::glmZ'-gfpmut3* λt₀ tet cat ori-pSC101</i>	this work
pYG272	<i>lacI^q P_{LacO-1}::glmZ'-cpxQ λt₀ tet cat ori-pSC101</i>	this work
pYG273	<i>lacI^q P_{LacO-1}::cpxQ λt₀ tet cat ori-pSC101</i>	this work
pYG274	<i>lacI^q P_{LacO-1}::glmZ'-ryhB λt₀ tet cat ori-pSC101</i>	this work
pYG275	<i>lacI^q P_{LacO-1}::ryhB λt₀ tet cat ori-pSC101</i>	this work
pYG276	<i>lacI^q P_{LacO-1}::glmZ'-sroC λt₀ tet cat ori-pSC101</i>	this work
pYG277	<i>lacI^q P_{LacO-1}::sroC λt₀ tet cat ori-pSC101</i>	this work
pYG313	<i>lacI^q P_{LacO-1}::glmZ'-micC λt₀ tet cat ori-pSC101</i>	this work
pYG314	<i>lacI^q P_{LacO-1}::micC λt₀ tet cat ori-pSC101</i>	this work
pYG315	<i>λattP aadA</i> operator-less <i>P_{lac}::ompD</i> (-69 to +1178) <i>neo ori-p15A</i>	this work

^a*ori*: origin of replication; *RBS*: ribosomal binding site, *MCS*: multiple cloning site.

Supplementary Table III. Oligonucleotides used in this study.

Name	Sequence ^{a, b, c}	Res.site	Position ^d
BG121	GCACGCGTGCACCAGCTGGTGGCCCCGGTAAC	Sall, PvuII	<i>glmS</i> -311 to -292
BG123	GCTCTAGACATATGACCTTCTGCATCAACAAC	XbaI	<i>glmS</i> 129 to 106
BG230	GTAGATGCTCATTCCATCTC		<i>glmZ</i> 1 to 20
BG231	CTAATACGACTCACTATAGGGAGAAAACAGGTCTGTATGACAAC		<i>glmZ</i> 172 to 152
BG287	TGCCTGGCGCCGTAG		<i>rrfD</i> 1 to 16
BG288	CTAATACGACTCACTATAGGGAGAGCCTGGCAGTTCCTAC		<i>rrfD</i> 118 to 102
BG397	TGGCTGCAGTCTAGATTATCATGGTTTACGTTTTCCAGCG	PstI, XbaI	<i>rapZ</i> 855 to 833
BG1307	GCACGCGTGCACAAAAGGAGACATGACATATGGTAC	Sall	<i>rapZ</i> 1 to 7
BG1316	CTCGTACTCATATGCCGACACCATCGAATGGTG	NdeI	pKES170 51 to 70
BG1318	GCCCTGCAGATAAATGTGAGCGGATAACATTGAC	PstI	pYG183 4174 to 4198
BG1319	TCCCCGGGATGCGCCGCGTGC GGCTGC	AvaI	pYG183 1430 to 1406
BG1337	GCGCTCGAGCTGCAGAACAGCTCATTT CAGAATATTTGAG	XhoI, PstI	pKES170 1264 to 1240
BG1345	CGCACCGGTCAAAGTCGGTGACAGATAACAGGAGTAAGTAATGCGTAAA GGAGAAGAACTTTTC	AgeI	<i>gfp_{mut3}</i> 1 to 24
BG1354	GCGTCTAGATTATTTGTATAGTTCATCCATGCCATGTG	XbaI	<i>gfp_{mut3}</i> 714 to 689
BG1399	AAATAAAAATTATACTTTTAAATTTGCTATACGTTATTCTGCGCGGTGTAGGC TGGAGCTGCTTCG		<i>micC</i> -45 to -1
BG1400	AGCAACCCGATTAATGCTCTGGATAAGGATTATCCAATTCTAATTACAT ATGAATATCCTCCTTAGTTCCTATT		<i>micC</i> 155 to 110
BG1455	GCGGGTACCCTGCAGTATTTGTAGAGCTCATCCATGCC	Acc56I, PstI	pXG10-SF
BG1456	GCGTCTAGAGGATCCGCTGGCTCCGCTGCTGGTTCTGGCGAATTCATGA GCAAAGGAGAAGAAGAACTTTTC	XbaI	pXG10-SF
BG1457	GCACCAGCTGTTGACAATTAATCATCGGCTCGTATAATGTGTGGAAGTGG CCCCGGTAACAGTAGG	PvuII	
BG1489	CGCACCGGTTCTCGCGATCAGGAAGACCCTC	AgeI	<i>ryhB</i> -4 to 18
BG1490	CTAATACGACTCACTATAGGGAGAGAATTCTAACGAACACAAGCACTCCC GTG	EcoRI	<i>ryhB</i> 140 to 117
BG1492	GGCCAAGACGTCGCGATCAGGAAGACCCTCGC	AatII	<i>ryhB</i> 1 to 20
BG1493	CGCACCGGTCTGTTTTCTTGGCCATAGACAC	AgeI	<i>cpxQ</i> -4 to 19
BG1494	CTAATACGACTCACTATAGGGAGAGAATTCAACGGAAGCAAATCATCTGC AATG	EcoRI	<i>cpxQ</i> 108 to 84
BG1496	GGCCAAGACGCTTTTTCTTGGCCATAGACACCATC	AatII	<i>cpxQ</i> 1 to 23
BG1497	CGCACCGGTGGCACTGAACCTAATTACAAGAACC	AgeI	<i>sroC</i> -4 to 20
BG1498	CTAATACGACTCACTATAGGGAGAGAATTCTTGTGTAATAAAAAATACCCCA GTTTC	EcoRI	<i>sroC</i> 213 to 187
BG1500	GGCCAAGACGTCCTGAACTAATTACAAGAACCAGGG	AatII	<i>sroC</i> 1 to 24
BG1501	CAAAAAGTGTGGACAAGTGCGAATGAGAATGATTATTATTGTCTCGTGTA GGCTGGAGCTGCTTCG		<i>ryhB</i> -46 to -1
BG1502	TAACGAACACAAGCACTCCCGTGGATAAATTGAGAACGAAAGATCAAAAA CATATGAATATCCTCCTTAGTTCCTATTCC		<i>ryhB</i> 141 to 91
BG1503	GTTGAAGCTATTGAGTAGTAGCAACTCACGTTCCAGTAGGTGTAGGCTG GAGCTGCTTCG		<i>cpxQ</i> -49 to -9
BG1504	GCAAATTGAGGATAAAAAAACCCACAGCATGTGGGGCATATGAATA TCCTCCTTAGTTCCTATTCC		<i>cpxQ</i> 71 to 31
BG1505	ATGAAAGCACTGTTCAAAGAACC GAATGACAAGGCACTGAACTAAGTGTA GGCTGGAGCTGCTTCG		<i>sroC</i> -40 to 9
BG1506	GACATAAATCTACTCCAGAAAAAGAGGGTAGCAGCGTAACTGCTACCC CATATGAATATCCTCCTTAGTTCCTATTCC		<i>sroC</i> 193 to 143
BG1513	GCGTCTAGATAACGAACACAAGCACTCCCGTG	XbaI	<i>ryhB</i> 140 to 117
BG1514	GCGTCTAGAAACGGAAGCAAATCATCTGCAATG	XbaI	<i>cpxQ</i> 108 to 84
BG1515	GCGTCTAGATTGTTGTAATAAAAAATACCCAGTTC	XbaI	<i>sroC</i> 213 to 187
BG1613	ACTTCTGAGCCGGAACGAAAA		<i>gcvB</i> 1 to 22
BG1614	CTAATACGACTCACTATAGGGAGATACATTAATCACTATGGACAGACA		<i>gcvB</i> 178 to 155
BG1615	CGATGTAAGACATCACTGCCGACGTAACAGGTTAAAGACTACA AAGACCATGACGG		<i>skp</i> 440 to 483
BG1616	TGCATCCAAGTCTGCGCTAAATCAGCCAGTCGAATTGAAGGCATATGAA TATCCTCCTTAGTTCCTATTCC		<i>lpxD</i> 45 to 1
BG1700	CGCACCGGTTCTTGTATATGCCTTATTGTACATATTC	AgeI	<i>micC</i> 1 to 27
BG1701	GGCCAAGACGTCGTTATATGCCTTATTGTACATATTC	AatII	<i>micC</i> 1 to 27
BG1702	CTAATACGACTCACTATAGGGAGATCTAGAGGAAAAACCCGGCGCAGATT AAA	XbaI	<i>micC</i> 159 to 136
BG1703	ATGTCATTGCAATTACCTGCAC		<i>sodB</i> 1 to 22

BG1704	<u>CTAATACGACTCACTATAGGGAGATTATGCAGCGAGATTTTCGC</u>		<i>sodB</i> 582 to 562
BG1705	<u>GCACGCGTCGACTTGACAATTAATCATCGGCTCGTATAATGTGTGGAA</u> <u>GCCATTGACAAACGCCTCGTT</u>	Sall	<i>ompD</i> -69 to -49
BG1720	<u>GGCCTGCAGCTGCACGGCATACTCCTTATG</u>	PstI	<i>ompD</i> 1178 to 1157
BG1727	<u>CTTCACCAAAGCGGCTAAAGTG</u>		<i>ompD</i> 1022 to 1044
BG1728	<u>CTAATACGACTCACTATAGGGAGAGCCCTGAAAGGACTGGCTTTG</u>		<i>ompD</i> 1129 to 1108
BG1797	<u>CGCACCGGTTCTTGTTATATGCCCCTATTGTCACATATTCATTTTGTGCG</u>	Agel	<i>micC</i> 1 to 10/13 to 37
BG1798	<u>GGCCAAGACGTCGTTATATGCCCCTATTGTCACATATTCATTTTGTGCG</u>	AatII	<i>micC</i> 1 to 10/13 to 37
BG1799	<u>ATGGAGATCTCCTGGGGCCG</u>		<i>nhaB</i> 1 to 20
BG1800	<u>CTAATACGACTCACTATAGGGAGACGGTGATAAATACCATAAAAACCG</u>		<i>nhaB</i> 500 to 476
BG1823	<u>CTAATACGACTCACTATAGGGAGAGTTATATGCCTTTATTGTCACATATTC</u>		<i>micC</i> 1 to 27
BG1824	<u>AAAAAAGCCCGAACATCCGTTCC</u>		<i>micC</i> 109 to 85
BG1973	<u>AAATAAAAATTATACAATATCATTTCGGTTACGATATTCTACGCCTGTGTAG</u> <u>GCTGGAGCTGCTTCG</u>		<i>S. T. micC</i> -45 to -1
BG1974	<u>AACCCGGCGCAGATTAATAAATATTCTAAGGATTAACCTGGAAACCATATG</u> <u>AATATCCTCCTTAGTTCC</u>		<i>S. T. micC</i> 110 to 155
BG2045	<u>CGCACCGGTTCTTGTTATATGCCTTTATTGTCACATATTC</u>	Agel	<i>micC</i> 1 to 27
BG2046	<u>CGCACCGGTTCTTGTTATATGCCTTTATTGTCACATATTC</u>	Agel	<i>micC</i> 1 to 27

^aRestriction sites are underlined. ^bRecognition sites for the T7 RNA polymerase promoter are underlined by dashed lines. ^cPositions deviating from the *wild-type* sequence are in bold. ^dPositions are relative to the first nucleotide of the respective gene as annotated in the EcoCyc database (15). S.T. = *Salmonella Typhimurium*.

SUPPLEMENTARY REFERENCES

1. Corcoran, C.P., Podkaminski, D., Papenfort, K., Urban, J.H., Hinton, J.C. and Vogel, J. (2012) Superfolder GFP reporters validate diverse new mRNA targets of the classic porin regulator, MicF RNA. *Mol. Microbiol.*, **84**, 428-445.
2. Sharma, C.M., Papenfort, K., Pernitzsch, S.R., Mollenkopf, H.J., Hinton, J.C. and Vogel, J. (2011) Pervasive post-transcriptional control of genes involved in amino acid metabolism by the Hfq-dependent GcvB small RNA. *Mol. Microbiol.*, **81**, 1144-1165.
3. Urban, J.H. and Vogel, J. (2008) Two seemingly homologous noncoding RNAs act hierarchically to activate *glmS* mRNA translation. *PLoS Biol.*, **6**, e64.
4. Baba, T., Ara, T., Hasegawa, M., Takai, Y., Okumura, Y., Baba, M., Datsenko, K.A., Tomita, M., Wanner, B.L. and Mori, H. (2006) Construction of *Escherichia coli* K-12 in-frame, single-gene knockout mutants: the Keio collection. *Mol. Syst. Biol.*, **2**, 1-11.
5. Venkatesh, G.R., Kembou Koungni, F.C., Paukner, A., Stratmann, T., Blissenbach, B. and Schnetz, K. (2010) BglJ-RcsB heterodimers relieve repression of the *Escherichia coli* *bgl* operon by H-NS. *J. Bacteriol.*, **192**, 6456-6464.
6. Morita, T., Kawamoto, H., Mizota, T., Inada, T. and Aiba, H. (2004) Enolase in the RNA degradosome plays a crucial role in the rapid decay of glucose transporter mRNA in the response to phosphosugar stress in *Escherichia coli*. *Mol. Microbiol.*, **54**, 1063-1075.
7. Kalamorz, F., Reichenbach, B., März, W., Rak, B. and Görke, B. (2007) Feedback control of glucosamine-6-phosphate synthase GlmS expression depends on the small RNA GlmZ and involves the novel protein YhbJ in *Escherichia coli*. *Mol. Microbiol.*, **65**, 1518-1533.
8. Reichenbach, B., Maes, A., Kalamorz, F., Hajnsdorf, E. and Görke, B. (2008) The small RNA GlmY acts upstream of the sRNA GlmZ in the activation of *glmS* expression and is subject to regulation by polyadenylation in *Escherichia coli*. *Nucleic Acids Res.*, **36**, 2570-2580.
9. Miyakoshi, M., Chao, Y. and Vogel, J. (2015) Cross talk between ABC transporter mRNAs via a target mRNA-derived sponge of the GcvB small RNA. *EMBO J.*, **34**, 1478-1492.
10. Hoiseth, S.K. and Stocker, B.A. (1981) Aromatic-dependent *Salmonella typhimurium* are non-virulent and effective as live vaccines. *Nature*, **291**, 238-239.
11. Nagarajavel, V. (2007) H-NS mediated repression of the *E.coli* *bgl* and *proU* operons. *Ph.D thesis; Institute for Genetics; University of Cologne, Germany.*
12. Lüttmann, D., Heermann, R., Zimmer, B., Hillmann, A., Rampp, I.S., Jung, K. and Görke, B. (2009) Stimulation of the potassium sensor KdpD kinase activity by interaction with the phosphotransferase protein IIA^{Ntr} in *Escherichia coli*. *Mol. Microbiol.*, **72**, 978-994.
13. Göpel, Y., Papenfort, K., Reichenbach, B., Vogel, J. and Görke, B. (2013) Targeted decay of a regulatory small RNA by an adaptor protein for RNase E and counteraction by an anti-adaptor RNA. *Genes Dev.*, **27**, 552-564.
14. Göpel, Y., Khan, M.A. and Görke, B. (2016) Domain swapping between homologous bacterial small RNAs dissects processing and Hfq binding determinants and uncovers an aptamer for conditional RNase E cleavage. *Nucleic Acids Res.*, **44**, 824-837.
15. Keseler, I.M., Mackie, A., Santos-Zavaleta, A., Billington, R., Bonavides-Martinez, C., Caspi, R., Fulcher, C., Gama-Castro, S., Kothari, A., Krummenacker, M. et al. (2017) The EcoCyc database: reflecting new knowledge about *Escherichia coli* K-12. *Nucleic Acids Res.*, **45**, D543-D550.